UvA-DARE (Digital Academic Repository)

Photoionization and photodissociation dynamics of H2 after (3+1) REMPI via the B state

Scheper, C.R.; Buma, W.J.; de Lange, C.A.; van der Zande, W.J.

Link to publication

Photoionization and photodissociation dynamics of H_2 after $(3+1)$ resonance-enhanced multiphoton ionization via the $B\ ^1\Sigma_u^+$ state

C. R. Scheper, W. J. Buma, and C. A. de Lange
Laboratory for Physical Chemistry, University of Amsterdam, Nieuwe Achtergracht 127–129, 1018 WS Amsterdam, The Netherlands

W. J. van der Zande
FOM-Institute for Atomic and Molecular Physics, Kruislaan 407, 1098 SJ Amsterdam, The Netherlands

We present a study of the molecular photoionization and photodissociation processes in molecular hydrogen occurring after one-photon absorption from various rovibrational levels ($v'=3-22$, $J' =0-3$) of the $B\ ^1\Sigma_u^+(1s\sigma_g)(2p\sigma_u)$ state using resonance-enhanced multiphoton ionization in combination with high-resolution photoelectron spectroscopy (REMPI-PES). For one-photon absorption from the $v'=3-8$ levels, molecular photoionization competes with photodissociation into a ground-state atom and an atom in an $n=2$ excited state. A detailed comparison of the photoelectron spectra obtained via different rotational branches and vibrational levels strongly indicates that singly excited bound $^1\Sigma_g^+$ and $^1\Pi_g$ Rydberg states at the four-photon level exert a significant influence on the final state distributions of H_2^+. In contrast, one-photon absorption from the $v'=9$ and higher levels leads almost exclusively to dissociation into a ground-state atom and an excited-state atom with $n>2$. Excited atomic fragments are ionized in a one-photon absorption step, and excited-atom distributions over the energetically allowed values of the principal quantum number n are obtained. Simulations of these distributions suggest that excitation of dissociative continua of bound $^1\Sigma_g^+(1s\sigma_g)(ns\sigma_g)$, $^1\Sigma_g^+(1s\sigma_g)(nd\sigma_g)$, and $^1\Pi_g(1s\sigma_g)(nd\pi_g)$ Rydberg states may dominate over excitation of dissociative doubly excited $^1\Sigma_g^+(2p\sigma_u)(np\sigma_u)$ and $^1\Pi_g(2p\sigma_u)(np\pi_u)$ states when considering the dissociation dynamics after one-photon absorption from the $v'\geqslant9$ levels of the B-state. © *1998 American Institute of Physics.* [S0021-9606(98)00243-8]

I. INTRODUCTION

In the last 5 years, dissociative recombination has been a subject of extensive and detailed studies. In this process, free electrons recombine with molecular ions resulting in the breakup of the molecule into fragments. For molecular hydrogen, dissociative recombination at low electron collision energies (<3 eV) can be pictured as proceeding in three stages: (i) electron capture into a doubly excited repulsive curve of the neutral molecule, (ii) competition between auto-ionization and dissociation along this curve, the so-called survival process, and (iii) a long-range half-collision/dissociation process of the neutral molecule leading to two fragments. The first two steps determine the electron capture cross section; the last stage is responsible for the final product state distributions. It is worth noting, that in spite of the apparent simplicity of molecular hydrogen, the half-collision process is very complicated. As described by Chupka[1] in a discussion of multiphoton dissociation of H_2, this process is affected by a large series of interactions between doubly excited repulsive states and singly excited bound molecular Rydberg states at large internuclear separations. This process distributes fragment flux over many outgoing channels. For a complete description, the couplings at each (avoided) crossing should be known and put in a multichannel treatment.[2] Many of the rather recent dissociative recombination experiments, especially on molecular hydrogen, have been performed in ion storage ring devices.[2–8] Although these experiments have enabled both (absolute) cross sections[3–6] and product state information[2,7,8] to be obtained, a description of the dissociation process is difficult because of the limited product state resolution of the imaging techniques employed in storage ring experiments.

The dissociation process is formally independent from the way the doubly excited state is formed. The dynamics of the dissociation process might therefore also be investigated through access of doubly excited states from below by a multiphoton absorption scheme. Indeed, REMPI experiments performed in the past via the $B\ ^1\Sigma_u^+$,[9–13] $C\ ^1\Pi_u$,[11,14–17] $EF\ ^1\Sigma_g^+$,[18–26] $B'\ ^1\Sigma_u^+$,[25,27] $B''\ ^1\Sigma_u^+$,[25] and $D\ ^1\Pi_u$[25,27] states have amply demonstrated the influence of these doubly excited states on the photoionization and photodissociation dynamics of the molecule. The distinct advantage of such a multistep laser excitation scheme is that laser ionization of excited hydrogen fragments affords a considerably better resolution in the final-state distribution.

In the present experiments the photoionization and photodissociation dynamics of molecular hydrogen have been investigated by $(3+1)$ REMPI via the $B\ ^1\Sigma_u^+(1s\sigma_g)(2p\sigma_u)$ ($v'=3-22;J'=0-3$) rovibrational levels, thereby probing in a stepwise manner the four-photon energy region between 125 000 and 150 000 cm^{-1} (15.5–18.6 eV). *A priori* considerations show that in these
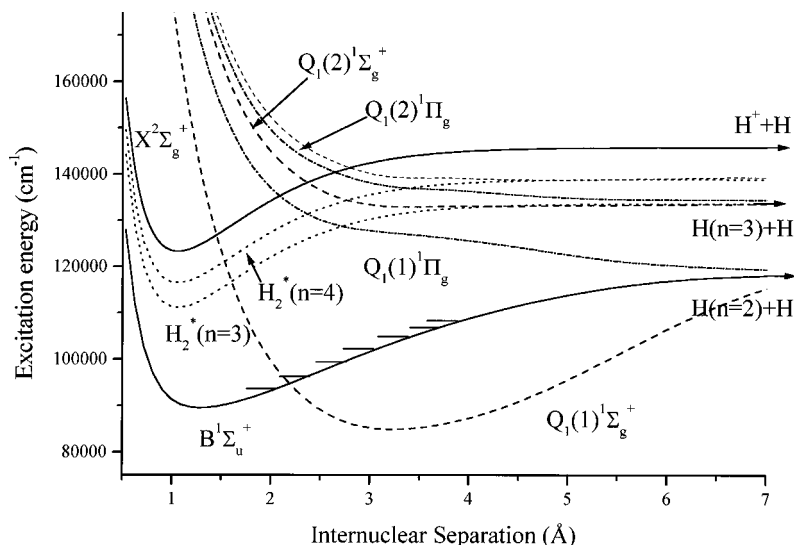
FIG. 1. Schematic potential energy diagram of molecular hydrogen. The $v'=3-22$ levels of the $B\ ^1\Sigma_u^+$ state, formed from the ground state with three photons, are dissociated or ionized using a one-photon excitation via the doubly excited repulsive Q_1-states[37] of $^1\Sigma_g^+$ (dashed lines) or $^1\Pi_g$ symmetry (dashed-dots) or via the dissociation continuum of bound Rydberg states, $[H_2^*\ (n=3)$ and higher, dotted lines]. A quasidiabatic representation is presented, ignoring the interactions between the Rydberg states and the doubly excited states. The $v'=3, 5, 8, 11, 14, 17,$ and 20 are indicated in the B-state.

experiments, one-photon absorption from the intermediate $B\ ^1\Sigma_u^+$ state may lead to various processes (Fig. 1). First, the molecule can ionize to various rovibrational levels of the ground ionic state $^2\Sigma_g^+(1s\sigma_g)$. Second, doubly excited states with a $(2p\sigma_u)(nl\lambda)$ configuration may be excited. These doubly excited states can (i) autoionize to the ground ionic state, or (ii) lead to dissociation of the molecule resulting in a ground-state hydrogen atom and an excited atom $H(n'l)$, where n' may differ from n. A final possibility, which has not been considered extensively in previous $(3+1)$ REMPI experiments via the $B\ ^1\Sigma_u^+$ state, is that the dissociation continua of singly excited bound Rydberg states of the type $(1s\sigma_g)(n''l\lambda)$ are excited. One of the aims of the present study is to elucidate the role of these states in the one-photon photoionization and dissociation dynamics of the $B\ ^1\Sigma_u^+$ state.

In our experiments, both molecular ionization and dissociation into a ground-state hydrogen atom and an excited fragment are observed. Under the employed experimental conditions, all excited fragments are ionized by further one-photon absorption. The identity of the excited atoms is established using kinetic-energy-resolved photoelectron spectroscopy with a resolution of about 10 meV, allowing principal quantum numbers from $n=2$ to $n=8$ to be distinguished. The same technique concurrently enables us to determine the internal energy distribution of the generated molecular ions with rotational resolution.

Our photoelectron spectra demonstrate that absorption from the $v'=3-8$ levels of the $B\ ^1\Sigma_u^+$ state leads to both molecular photoionization and photodissociation into an $H(n=1)$ and $H(n=2)$ pair, the only accessible limit in this energy region. The observed distributions over the rovibrational levels of the molecular ion give evidence for the importance of singly excited Rydberg states located at the four-photon level in the proper description of the molecular photoionization dynamics. For absorption from $v'\geqslant 9$ levels of the $B\ ^1\Sigma_u^+$ state, mostly photodissociation fragments are observed. The distributions over the possible values of the principal quantum number n observed for absorption from the $v'=9-22$ levels will be discussed in the light of two

models, one in which photodissociation occurs exclusively on the potential energy surfaces of doubly excited states, and another in which the dissociative continua of singly excited Rydberg states are responsible for photodissociation.

II. EXPERIMENT

The experimental setup has been described in detail previously.[28] Briefly, the laser system consists of a Lumonics HyperDye-500 dye laser (bandwidth ~0.08 cm^{-1}) operating on Rhodamine B, Rhodamine 6G, or Coumarin 540A, which is pumped by an XeCl excimer laser (Lumonics HyperEx-460) operating at 30 Hz. The dye laser output is frequency doubled in a Lumonics HyperTrak 1000 unit using a BBO or KD*P crystal, resulting in 10 ns pulses with a maximum energy of about 15 mJ. The laser light is focused into the ionization region of a ''magnetic bottle'' spectrometer by a quartz lens with a focal length of 25 mm. Electrons are collected with an efficiency of about 50%. Analysis of their kinetic energies is performed with a time-of-flight technique allowing an energy resolution of about 10 meV at all kinetic energies. The energy scale was calibrated using $(3+1)$ REMPI via well-known excited states of krypton.[29]

In the ionization chamber of the spectrometer, two grids are installed which enable the application of dc or pulsed electric fields. In the case of excitation via the $v'=3-8$ vibrational levels of the B state, a negative static field $(-10$ V/cm) was used in order to detect the very slow electrons formed in direct ionization processes. Apart from (kinetic-energy-resolved) electron detection, the spectrometer can also be employed in a mass-resolved ion detection mode by application of appropriate voltages to the grids in the ionization region. Used in the latter way, the spectrometer has, however, a lower collection efficiency.

H_2 (99.9995%, Air Liquide) was effusively introduced into the spectrometer.

III. RESULTS AND DISCUSSION

Three-photon excitation spectra of the $B\ ^1\Sigma_u^+$ state were obtained by scanning the laser wavelength and by monitor-
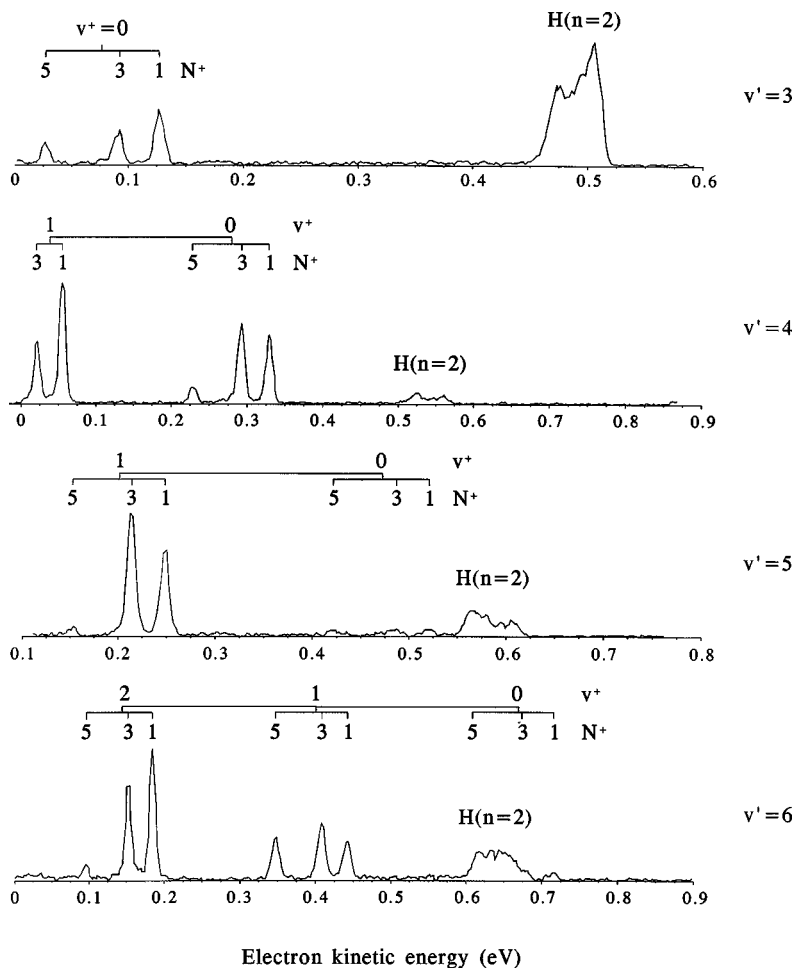
J. Chem. Phys., Vol. 109, No. 19, 15 November 1998

Scheper *et al.* 8321

FIG. 2. MPI-photoelectron spectra obtained following three-photon excitation of the $B\ ^1\Sigma_u^+$ ($v'=3-22$) levels via the $R(1)$ rotational transitions.

ing either the H^+ and H_2^+ ion channels, or an energy-selected part of the electron current. The measured positions of these resonances were found to be in good agreement with the data of Wilkinson,[30] Dabrowski and Herzberg,[31] and Namioka.[32] Photoelectron spectra were recorded for ionization via several rotational branches. The spectra obtained for ionization after excitation of the $v'=3-22$ vibrational levels via the $R(1)$ transition are shown in Fig. 2.

Inspection of the spectra depicted in Fig. 2 clearly shows that the absorption of an additional photon from $B\ ^1\Sigma_u^+(v')$ levels leads to a number of competing processes. The photoelectron spectra obtained for ionization via $B\ ^1\Sigma_u^+$ vibrational levels up to $v'=8$, for instance, are dominated by peaks arising from a molecular photoionization process yielding H_2^+ in the various accessible vibrational (v^+) and rotational (J^+) levels of its electronic ground ionic state $X\ ^2\Sigma_g^+$. Apart from molecular ionization, a competing dissociation process leading to excited $H(n=2)$ atoms, which are subsequently ionized by one-photon absorption, is also visible in these spectra. The width of the $H(n=2)$ peak is due to the large kinetic energy of the H fragments, ≈ 0.9 eV/H-atom.

For ionization via the vibrational levels up to $v'=8$, dissociation plays a minor role, a situation which changes dramatically when ionization is performed via higher vibrational levels. Figure 2 shows that, above the $n=3$ threshold ($v'>8$), dissociation in fact dominates over direct ioniza-

tion of molecular hydrogen, in agreement with previous results.[10] The photoelectron spectra for ionization via $v'=14$ and 16 might seem to be at odds with this conclusion, since they exhibit rather large peaks on the low-energy side, which result from molecular ionization. However, these higher H_2^+ yields can be explained by the observation that the $R(1)$ transitions to the $v'=14$ and 16 levels are nearly coincident with the three-photon transitions to the $C\ ^1\Pi_u$ ($1s\sigma_g$)($2p\pi_u$) $v'=3$ and 4 levels, respectively. As demonstrated previously[11,14] and confirmed by the present experiments, one-photon absorption from the $C\ ^1\Pi_u$ state leads predominantly to molecular photoionization, with the dissociation pathway playing only a very minor role. The "slow" photoelectrons observed for $v'=14$ and 16 should consequently be attributed to molecular photoionization via the $C\ ^1\Pi_u$ state, while the excited hydrogen atoms result predominantly from excitation of the $B\ ^1\Sigma_u^+$ state. Apart from photoelectrons deriving from these two processes, the $v'=14$ and 16 spectra also show signals at 2.05 and 2.12 eV, respectively. These signals are not connected with ionization of molecular or atomic hydrogen, since they did not vanish when the hydrogen gas inlet was closed. The origin of these peaks is not understood.

In the following, we shall first discuss the molecular photoionization process, which can be observed for ionization via the vibrational levels up to $v'=9$. Subsequently, the dissociation process will be considered.
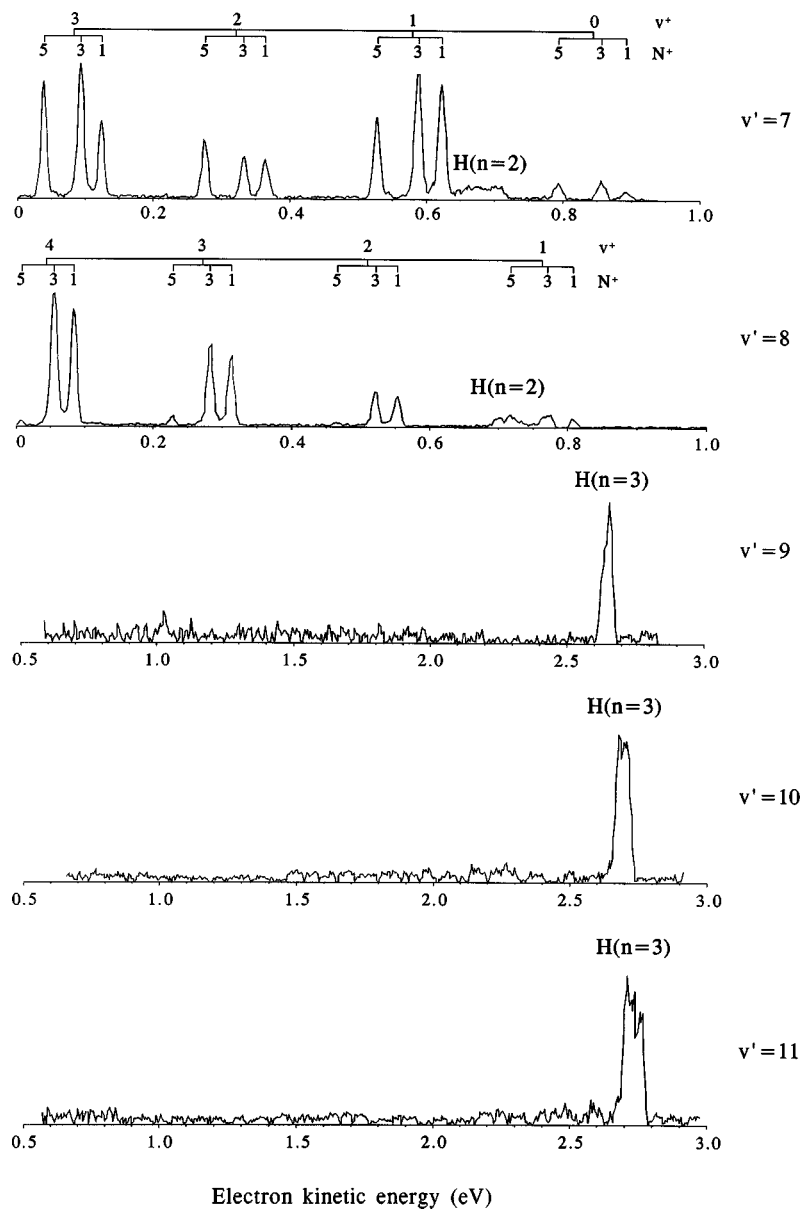
FIG. 2. (*Continued.*)

Electron kinetic energy (eV)

A. Molecular photoionization

For ionization via the $v'=3-8$ levels of the $B\ ^1\Sigma_u^+$ state, the photoelectron spectra exhibit well-resolved rotational structure in the transitions deriving from molecular photoionization to the various accessible vibrational levels in the ionic state. Comparable structure, though far less resolved, has been observed by Pratt *et al.*[9] for ionization via the $R(3)$ and $P(3)$ transitions to the $v'=7$ level. Rotational selection rules predict that in the one-photon ionization process from $B\ ^1\Sigma_u^+(v')$ levels, only $\Delta N+\ell=odd$ transitions should be allowed, where $\Delta N=N^+-N'$ and ℓ is a partial wave component of the photoelectron.[33] In an atomic-like picture, ionization of the $2p\sigma_u$ electron is expected to lead to $s(\ell=0)$ and $d(\ell=2)$ partial waves. Accordingly, only $\Delta N=odd$ transitions should be present in the photoelectron spectra. In the $B\ ^1\Sigma_u^+$ state, ortho-hydrogen can only exist in the $N'=0,2,4...$ and para-hydrogen only in the $N'=1,3,5...$ rotational levels. In the ionic $X\ ^2\Sigma_g^+$ state, ortho-hydrogen has only $N^+=1,3,5...$ and para-hydrogen only $N^+=0,2,4,...$

available to it. Therefore, in our experiments the photoelectron spectra show either formation of odd or even N^+ levels, due to ionization of ortho-or para-hydrogen, respectively.

Conservation of total angular momentum requires that s partial waves are accompanied by $\Delta N=\pm1$, while d partial waves may lead to changes of ±1 and ±3. In the first instance, one might be tempted to derive the relative importance of the s and d partial waves from the intensities of the $\Delta N=\pm1$ and ±3 transitions. The results of an *ab initio* study by Lynch *et al.*[34] of the rovibrational branching ratios resulting from $(3+1)$ REMPI via the $v'=7$ level of the $B\ ^1\Sigma_u^+$ state have shown, however, that such an approach is not valid. Here it was found that $\Delta N=\pm3$ transitions are largely suppressed as a result of dynamic interference between the $d\sigma$ and $d\pi$ channels, even though the d partial wave is in fact stronger than the s partial wave. As a result, the photoelectron spectra measured for ionization via the $R(3)$ and $P(3)$ transitions to the $v'=7$ level only exhibit $\Delta N=\pm1$ peaks.
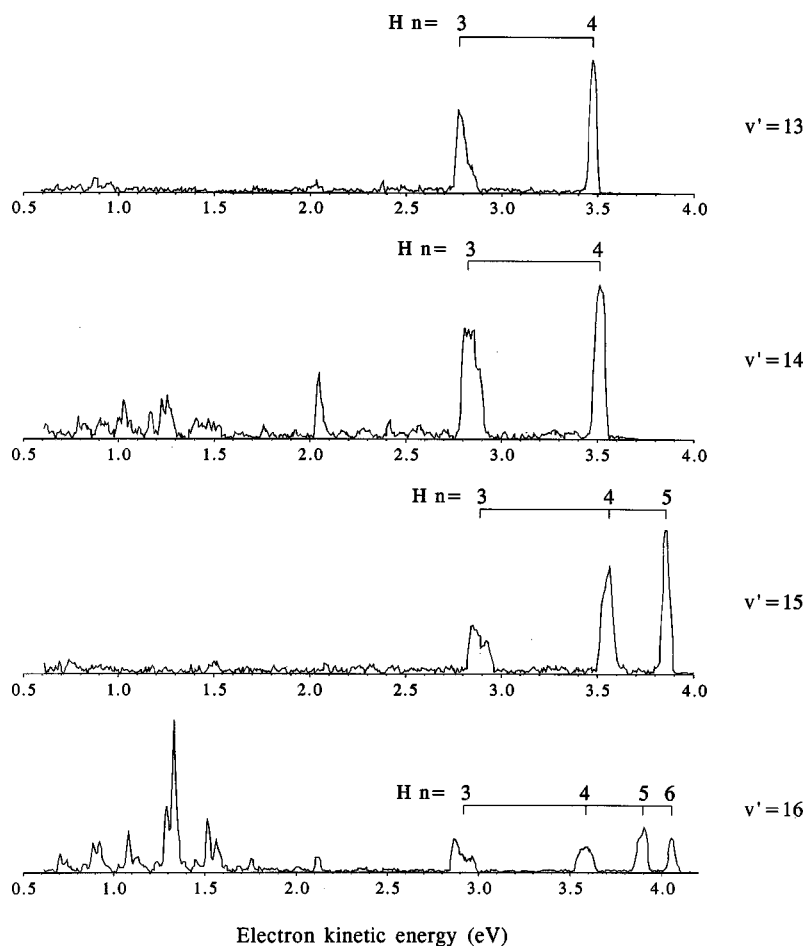
FIG. 2. (*Continued.*)

The photoelectron spectra obtained in the present study for ionization via the $v'=3-8$ levels of the $B\ ^1\Sigma_u^+$ state demonstrate that the ionization dynamics as observed and calculated previously for ionization via the $P(3)$ and $R(3)$ transitions to the $v'=7$ level are by no means exemplary for the other transitions. For example, Fig. 2 shows that for ionization via the $R(1)$ transition to the $v'=3-6$ and $v'=8$ levels, $\Delta N=\pm 3$ transitions are much weaker than the $\Delta N=\pm 1$ transitions, but are of similar intensity for $v'=7$. Analogous behaviour occurs for ionizing transitions via the $P(1)$ transition to the various vibrational levels in the excited state (not shown); ionization via the $v'=7$ level leads to dominant intensity in the $\Delta N=\pm 3$ transitions, while these peaks are significantly less intense for ionization via other vibrational levels.

Surprisingly, the intensities of $\Delta N=\pm 3$ transitions depend not only on the initial vibrational level in the excited state, but also on the rotational level, as well as the rotational branch employed to populate this rotational level. Consider, for example, the spectra measured for ionization via the $v'=7$ level (Fig. 3). Ionization via the $P(1)$, $R(1)$ and, to a lesser extent, $R(0)$ transitions results here in significant intensities of the $\Delta N=\pm 3$ transitions, while ionization via the $R(2)$, $R(3)$,[9] and $P(3)$[9] transitions leads to dominant $\Delta N=\pm 1$ transitions. These observations are even more peculiar when it is realized that the $R(1)$ transition, for which intense $\Delta N=\pm 3$ peaks are observed, populates the same rotational level in the excited state as the $P(3)$ transition, where ΔN $=\pm 3$ transitions are completely absent. Although the two rotational branches lead to a different alignment of the J' $=2$ level, one does not expect such large differences in ionization dynamics solely on the basis of a different initial alignment.

A final striking observation is that also, the vibrational branching ratios upon ionization may depend strongly on the rotational transition used to excite a particular vibrational level in the excited state. This is most apparent for ionization via the $v'=4$ level (Fig. 4). A previous study[13] found in this case that ionization via the $R(0)$ and $P(1)$ transitions leads to dominant population of the $v^+=1$ level, while ionization via the $R(1)$ transition results in equal intensities of the v^+ $=0$ and $v^+=1$ peaks. In the present study, these observations are supported and extended. Ionization via the $P(2)$ and $R(3)$ transitions leads to a small $v^+=0:v^+=1$ vibrational branching ratio; ionization via the $R(2)$ transition leads to a large ratio. Moreover, we observe that a large $v^+=0:v^+=1$ branching ratio is accompanied by a significant reduction of excited $H(n=2)$ fragments. Interestingly, when the photoelectron spectra are considered in order of the final energies reached in these experiments at the four-photon level, i.e., $P(2)$, $P(1)$, $R(0)$, $R(1)$, $R(2)$, and $R(3)$, it is clear that the $v^+=0:v^+=1$ branching ratio and the amount of dissociation do not vary randomly, but show a maximum and minimum, respectively, around $127\,100-127\,150$ cm^{-1}.

All of the above observations indicate that the ionization

H n=   3   4   5   6 7 8   v' = 17

2.7   3.2   3.7   4.2   4.7

H n=   3   4   5   6   7   14   v' = 18

2.7   3.2   3.7   4.2   4.7

H n=   3   4   5   6   ∞   v' = 19   FIG. 2. (Continued.)

2.7   3.2   3.7   4.2   4.7

H n=   3   4   5   6   ∞   v' = 21

2.6   3.1   3.6   4.1   4.6

       3   4   5   6   ∞   v' = 22

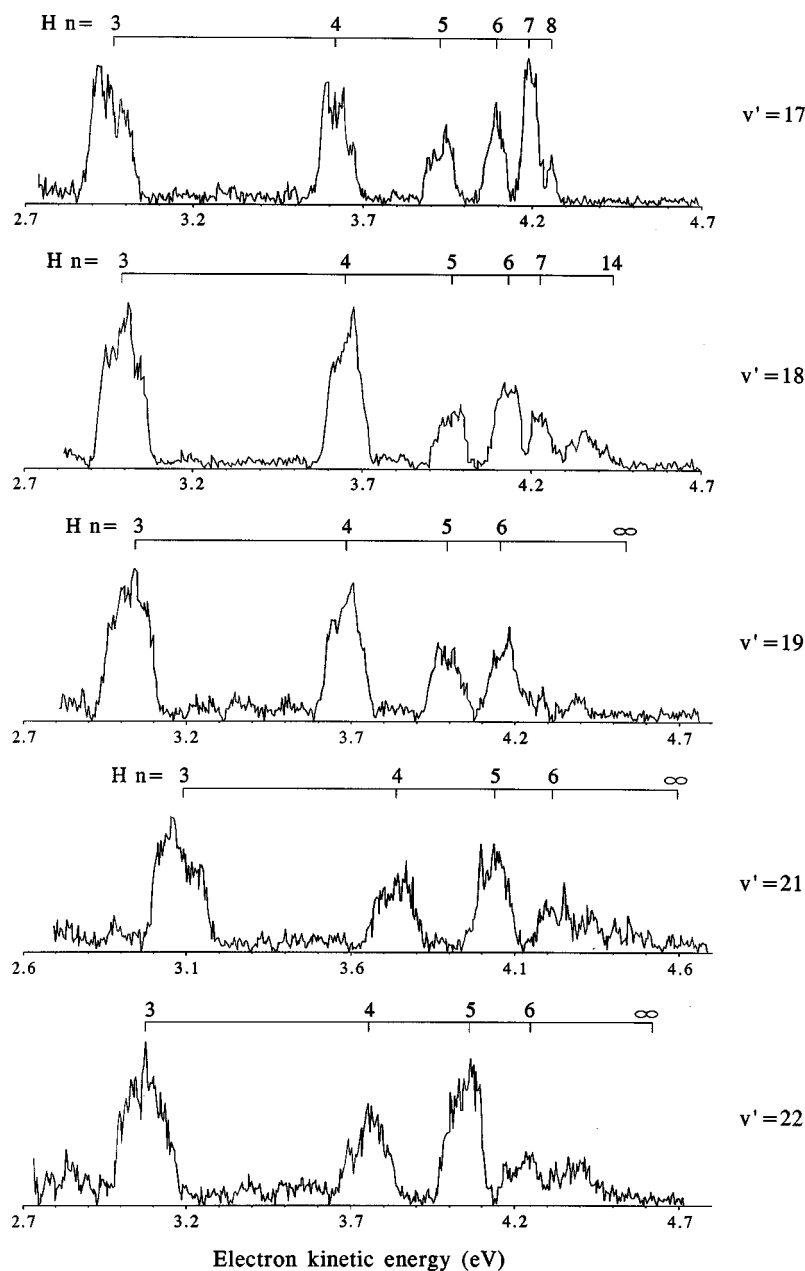2.7   3.2   3.7   4.2   4.7

Electron kinetic energy (eV)

dynamics depend sensitively on the *four-photon* level reached in the experiments. *Ab initio* calculations have shown that dynamic interference between the $d\sigma$ and $d\pi$ ionization channels plays an important role in describing ionization from the $B\ ^1\Sigma_u^+(v'=7)$ level.[34] The delicate balance between these two channels will certainly be electron-kinetic-energy dependent, but it is hard to imagine that this energy dependence would be so large that a mere change of a few $100\ \mathrm{cm}^{-1}$ in kinetic energy, as is occurring, for example, when ionizing via the $R(1)$ or the $P(3)$ transition to the $v'=7$ level, would make so much difference. Another possible explanation might be found in the influence of dissociative Rydberg states converging upon the $^2\Sigma_u^+(2p\sigma_u)$ ionic state. For excitation of the levels investigated here, the only doubly excited states that can be accessed at the four-photon level are the $^1\Sigma_g^+(2p\sigma_u)^2$ and $^1\Pi_g(2p\sigma_u)(2p\pi_u)$ Rydberg states. Calculations of the Franck-Condon factors between the vibrational wavefunctions of $B\ ^1\Sigma_u^+(v')$ levels

and these dissociative $^1\Sigma_g^+$ and $^1\Pi_g$ states show that these factors do not vary enough to account for the observed rotational branch dependence of one particular $B\ ^1\Sigma_u^+(v')$ level. These doubly excited states might, however, be involved in an explanation of the v'-dependence of the photoelectron spectra (*vide infra*), which involve a much larger range of energy.

The fact that features observed in the photoelectron spectra change so drastically over a relatively small energy interval strongly suggests that bound states at the four-photon level are of influence. At this energy level, vibrationally excited Rydberg states with a $X\ ^2\Sigma_g^+(1s\sigma_g)$ ionic core are present, which converge upon v^+ levels of the ground ionic state that lie higher in energy than the employed four-photon energy. From the point of view of vibrational overlap these levels are well accessible, since the potential energy surface of the $B\ ^1\Sigma_u^+$ state is significantly different from that of the bound Rydberg states. Upon exci-
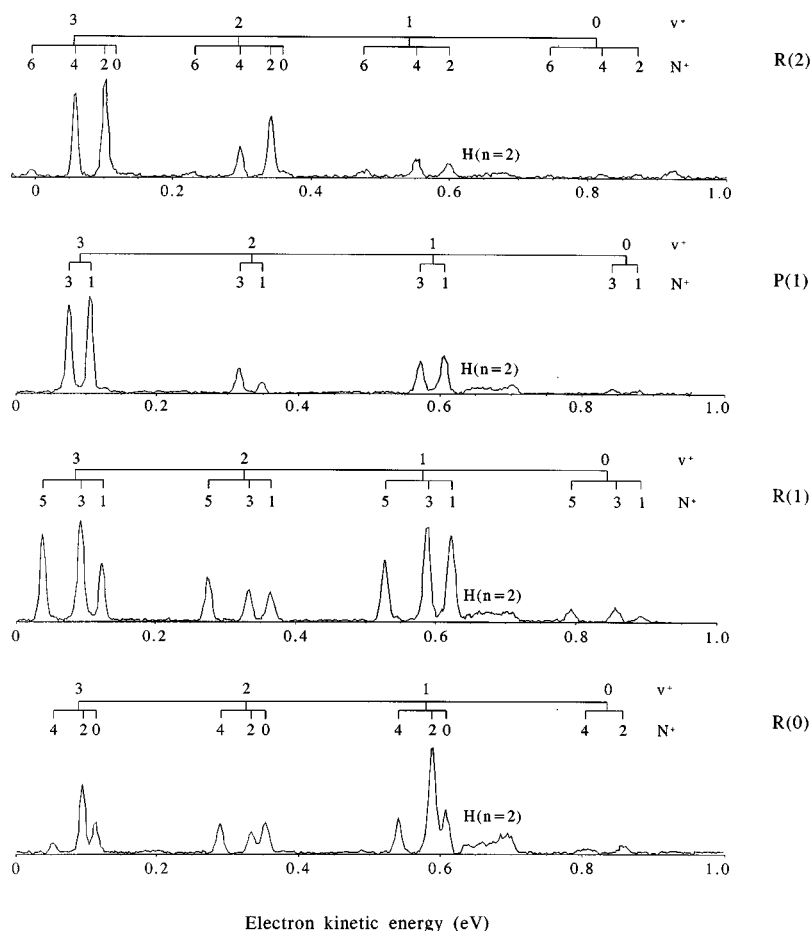
FIG. 3. MPI-photoelectron spectra obtained following three-photon excitation of the $B\ ^1\Sigma_u^+$ ($v'=7$) level via various rotational transitions.

tation of these states, the photoelectron spectra will not merely display the photoionization dynamics of the $B\ ^1\Sigma_u^+$ state, but also the decay dynamics of the bound Rydberg state. A complete unraveling of the influence of bound Rydberg states on the molecular photoionization spectra clearly demands, theoretically, the application of high-quality *ab initio* calculations. In addition, experimental studies, in which $B\ ^1\Sigma_u^+(v')$ levels are excited by one-photon absorption and subsequently ionized in a tunable one-photon absorption step, would be most welcome.

B. Photodissociation

Figure 2 shows that dissociation occurring at the four-photon level plays an important role in the one-photon excitation dynamics from the $B\ ^1\Sigma_u^+$ state. After one-photon absorption from the $v'=3$ to $v'=17$ levels, excited hydrogen atoms—on energy grounds accompanied by ground-state hydrogen atoms—are seen to be formed in all accessible Rydberg states. One notable exception concerns the $n=2$ fragments, which disappear as soon as the $n=3$ dissociation channel becomes accessible. Energetically, one-photon absorption from the next vibrational level ($v'=18$) allows dissociation into an excited hydrogen atom with $n<15$ and a ground-state hydrogen atom, whereas dissociation into all values of n is possible for absorption from higher vibrational levels. Not all of these states are actually observed: the photoelectron spectrum obtained via the $v'=18$ level shows

well-resolved peaks up to $n=7$, with a remaining peak covering the region from $n=8$ to $n=14$. For spectra recorded via $v'>18$ levels well-resolved peaks are obtained for excited hydrogen atoms with $n<6$, while an unresolved peak extends to about $n=11$.

It is the purpose of this section to rationalize the observed $H(n)$ distributions. These distributions reflect quantitatively the number of atoms formed in the various Rydberg states, i.e., we have to verify that all excited fragments present are ionized. The atomic photoionization cross section is proportional to n^{-3} and to $\nu^{-\ell-7/2}$ where ν is the photon frequency.[35] The disappearance of the signal in the photoelectron spectra at kinetic energies below the $n=\infty$ limit could be a consequence of the fact that the ionization cross section strongly decreases with increasing principal quantum number. In order to test this hypothesis, ionization cross sections have been estimated for a number of values of n and ℓ at a wavelength of $37\,000$ cm^{-1} using the Born approximation[35] and using analytical wavefunctions. Both methods are found to give cross sections of the same order of magnitude. Combination of these cross sections with the employed photon flux (10^{25} photons/m$^2\cdot$pulse for an energy of 1 mJ/pulse at 270 nm) then leads us to conclude that ionization of $H(n=11)$ is saturated under the present experimental conditions, if it is assumed that no fragments with $\ell>4$ are formed. The influence on the ionization yield of the 1 T magnetic field in the ionization chamber of the spectrometer
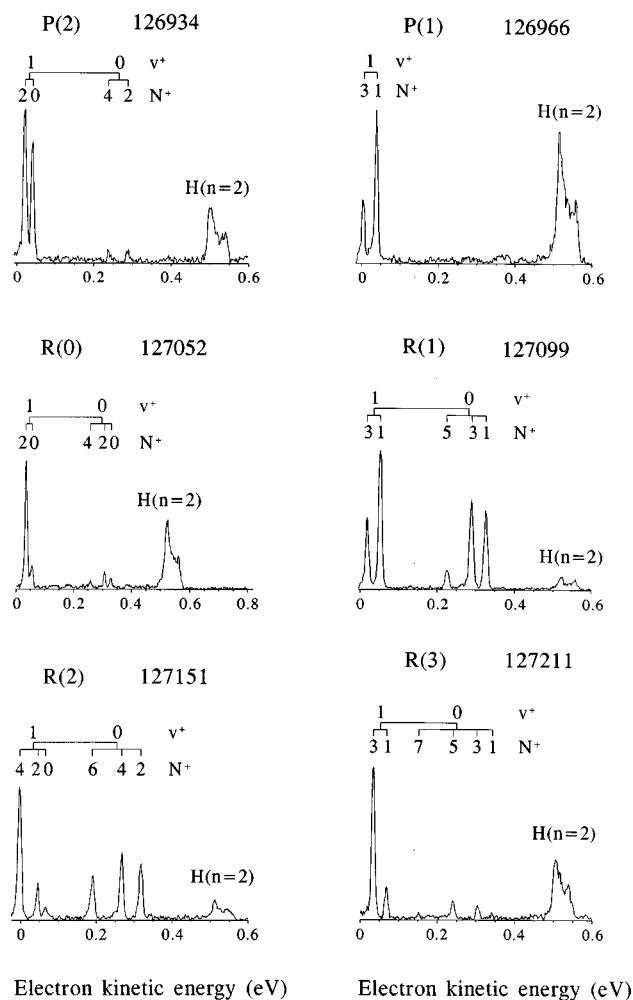
FIG. 4. MPI-photoelectron spectra obtained following three-photon excitation of the $B\ ^1\Sigma_u^+$ ($v'=4$) level via various rotational transitions. The final energy (cm^{-1}) reached at the four-photon level is given for each rotational transition.

FIG. 5. Experimentally obtained excited-atom H(n) distributions, estimated by calculating peak areas of the various fragments in the photoelectron spectra obtained following three-photon excitation of the $B\ ^1\Sigma_u^+$ ($v'=9$–22) levels via the $R(1)$ rotational transitions.

can be ruled out, since it becomes important only at much higher principal quantum numbers.[36] The observation that not all of the energetically allowed values of n are observed in the photoelectron spectra via $v'>18$ levels can thus *not* be attributed to experimental conditions. Other points of concern might be the short radiative lifetimes of H($2p$) and H($3p$) fragments (1.6 and 5.4 ns, respectively[23]), and the large kinetic energies of $n=2$ atoms, which could result in the disappearance of these fragments out of the focal volume before being ionized. The cross sections for ionization of H($2s$), H($2p$), and H($3p$), obtained at 30 000 cm^{-1} by using analytical wavefunctions, are $9.3\cdot10^{-20}$, $1.1\cdot10^{-19}$, and $2.5\cdot10^{-20}$ m^2, respectively. These cross sections, combined with the employed photon flux, give rise to such high ionization rates for H($n=2$) and H($n=3$) fragments that they can all be assumed to become ionized. We therefore conclude that quantitative excited-atom distributions can indeed be derived from the photoelectron spectra obtained in the present study. By calculating peak areas, excited-atom distributions have been obtained, which are depicted in Fig. 5.

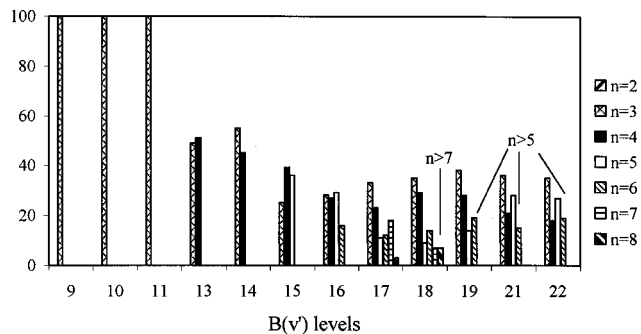Figure 5 reveals that most energetically allowed disso-

ciation limits are observed with the clear exception of the H($n=1$)+H($n=2$) dissociation limit as soon as the production of H($n=3$) is possible. A quantitative analysis of these distributions is very complex. A logical starting point forms a calculation of the relative excitation probabilities of the different doubly excited repulsive states. These states have Rydberg character and converge to the first excited state in H_2^+, the $^2\Sigma_u^+$ state (see Fig. 1). The correlation of these states with the various dissociation limits is nontrivial. The presence of the bound Rydberg series results in a large number of (avoided) crossings. Part of the double-well structures found in Born-Oppenheimer calculations of the $^1\Sigma_g^+$ Rydberg states is caused by the doubly excited repulsive character (see also Ref. 2). Due to these interactions, dissociation flux will be distributed over more than one dissociation limit even if one doubly excited state is excited in the Franck–Condon region.

We have decided to model the excited atom distributions in two separate calculations: (i) on the basis of cross sections for excitation of the doubly excited repulsive states, described in an uncoupled diabatic representation, and (ii) on the basis of cross sections to the dissociation continuum of singly excited Rydberg states. Both calculations describe, in zeroth order, a one-electron transition ($n\ell\lambda_u\leftarrow1s\sigma_g$) for the excitation to the doubly excited states, and ($n\ell\lambda_g\leftarrow2p\sigma_u$) for the singly excited Rydberg states.

(1) $X\ ^2\Sigma_g^+$ The relative transition probabilities have been calculated for excitation from the $B\ ^1\Sigma_u^+(v')$ levels to the accessible, $^1\Sigma_g^+(2p\sigma_u)(np\sigma_u)$ and $^1\Pi_g(2p\sigma_u)(np\pi_u)$, repulsive states with dissociation limits up to $n<7$. We calculated the integrals $\int\chi_k(R)D(R)\chi_{v'}(R)dR$, where $\chi_k(R)$ is the energy-normalized-nuclear wave function in the doubly excited state under consideration, $\chi_{v'}(R)$ the vibrational wave function of the $B\ ^1\Sigma_u^+(v')$ level, and $D(R)$ the one-photon electronic transition moment. The potential energy curves for the $Q_1\ ^1\Sigma_g^+$ states with H($n=1$)+H($n=2$) and H($n=1$)+H($n=3$) dissociation limits were taken from Gubermann.[37] The higher $^1\Sigma_g^+$ states are simply obtained by raising the R-dependent quantum defect of the $^1\Sigma_g^+$ state with the H($n=1$)+H($n=3$) dissociation limit with one for each successive state. The potential energy curves of the $^1\Pi_g$ states are calculated using the R-dependent quantum defect
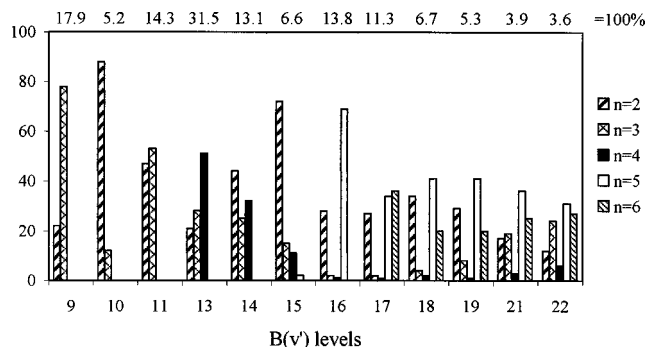
FIG. 6. Excited-atom distributions H(n) calculated for excitation via the $B\ ^1\Sigma_u^+(v')$ levels, and assuming that dissociation uniquely occurs by excitation of repulsive doubly excited states with $^1\Sigma_g^+(2p\sigma_u)(np\sigma_u)$ and $^1\Pi_g(2p\sigma_u)(np\pi_u)$ symmetry. For dissociation via each vibrational level, the sum of the cross sections for the pathways leading to H($n=2$) to H($n=6$) is set to 100% in the stick diagrams. The absolute value of this sum is given at the top of the diagram for each vibrational level.

of the $^1\Pi_g$ state with the H($n=1$)+H($n=2$) dissociation limit. Calculations on the relevant electronic transition moment have not been published. In the one-electron approximation this transition moment is given by the $\langle 1s\sigma_g|\vec{z}|2p\sigma_u\rangle$ matrix element. These matrix elements are also the dominant contribution to the $X\ ^1\Sigma_g^+(1s\sigma_g)^2 \rightarrow B\ ^1\Sigma_u^+(1s\sigma_g)(2p\sigma_u)$ transition and the $X\ ^1\Sigma_g^+(1s\sigma_g)^2 \rightarrow C\ ^1\Pi_u(1s\sigma_g)(2p\pi_u)$. The $X-B$ and $X-C$ transition moments may approximate the *magnitude* of the transition moments from the B state to the doubly excited states. The approximation becomes highly questionable at larger internuclear distances where the electronic character of the involved states changes. These arguments, and the calculated internuclear distance dependence of the calculated $X-B$ and $X-C$ electronic transition moments,[38] led us to use transition moments, independent of internuclear distance, of 1.6 a.u. and 1.0 a.u. for the $^1\Sigma_g^+(2p\sigma_u)^2 \leftarrow B\ ^1\Sigma_u^+(1s\sigma_g)(2p\sigma_u)$ and $^1\Pi_g(2p\sigma_u)(2p\pi_u) \leftarrow B\ ^1\Sigma_u^+(1s\sigma_g)(2p\sigma_u)$ transitions. For transitions to the higher doubly excited states, the electronic transition moments can be scaled by $(n^*/n^{**})^{3/2}$, where n^* is the effective quantum number of the $^1\Sigma_g^+(2p\sigma_u)^2$ or $^1\Pi_g(2p\sigma_u)(2p\pi_u)$ state, and n^{**} is the effective quantum number of the higher doubly excited state.

The distributions simulated with the above model are shown in Fig. 6. An important conclusion is that the higher-lying repulsive $^1\Sigma_g^+$ and $^1\Pi_g$ states are excited from the higher vibrational levels. Comparison of the simulated and experimentally obtained distributions shows poor agreement. In particular, the simulations predict that the H($n=2$) fragments should form an important exit channel. Simulations based upon R-dependent $X-B$ and $X-C$ transition moments do not improve the qualitative picture at all. From these results, in which interactions between doubly excited repulsive and singly excited bound Rydberg states have been neglected, one may conclude that the lowest $^1\Sigma_g^+(2p\sigma_u)^2$ doubly excited state correlates effectively with the H($n=1$)+H($n=3$) limit.

Recent results on low-energy electron collisions with H_2^+ (dissociative recombination) show that at total energies

above the H($n=3$) energy, a significant fraction of H($n=2$) fragments is still found.[2] The theoretical treatment in that paper implies that the lowest $Q_1\ ^1\Sigma_g^+$ state produces a significant fraction of H($n=2$) fragments at energies above the H($n=3$) limit.[2] The absence of H($n=2$) fragments in the present experiments has to be due to a mechanism other than direct excitation of the doubly excited repulsive states.

(2) The rapidly changing dynamics in the excitation from the lower B-state vibrational levels were indicative for the influence of vibrationally excited levels of singly excited Rydberg states on molecular photoionization. This inspired us to calculate the influence of the *vibrational continua* of singly excited Rydberg states with $^1\Sigma_g^+(1s\sigma_g)(ns\sigma_g)$, $^1\Sigma_g^+(1s\sigma_g)(nd\sigma_g)$, and $^1\Pi_g(1s\sigma_g)(nd\pi_g)$ symmetry on the final fragment-state distribution. As mentioned earlier, these states can be accessed by one-photon absorption from the $B\ ^1\Sigma_u^+$ state. We note that the potential energy curves of the $B\ ^1\Sigma_u^+$ state differ considerably from the bound Rydberg states. Hence, the overlap between the vibrational wavefunctions of $B\ ^1\Sigma_u^+(v')$ levels and the vibrational continua is not necessarily much smaller than the vibrational overlap for transitions to doubly excited repulsive Rydberg states. Also, the $2p\sigma_u \rightarrow (ns\sigma_g, nd\sigma_g, nd\pi_g)$ electronic transition moments are not expected to differ by orders of magnitude from the $1s\sigma_g \rightarrow (np\sigma_u, np\pi_u)$ electronic transition moments involved in the transition to doubly excited states. Excitation of these states has been ignored in previous studies on the $B\ ^1\Sigma_u^+$ state, even though it was concluded to be important in one-photon excitation studies from the $EF\ ^1\Sigma_g^+$ state.[26]

To put these arguments on a more quantitative basis, we have calculated the transition moments to the vibrational continua of $n=2$ and higher Rydberg states. As we observe hydrogen fragments, it is assumed that an $n=n'$ Rydberg state correlates with an excited H($n=n'$) fragment. Model bound Rydberg states have been made, assuming an R-independent integral quantum defect (see Fig. 1). Constant electronic transition moments have been assumed. We have used the electronic transition moments calculated for the $GK\ ^1\Sigma_g^+(1s\sigma_g)(3d\sigma_g) \leftarrow B$ and $H\bar{H}\ ^1\Sigma_g^+(1s\sigma_g)(3s\sigma_g) \leftarrow B$ transitions by Wolniewicz and Dressler[39] taken at the equilibrium separation of the B-state. Lynch *et al.*[34] calculated for ionization of the $B\ ^1\Sigma_u^+$ state that the electronic transition moments to the $\varepsilon s\sigma$ and $\varepsilon d\sigma$ continua are in the ratio of about 1:7. Since this corresponds to excitation of $n=\infty$ states, we assume that this ratio is equally applicable to the presently considered states. Support for this assumption is found in the calculations of Wolniewicz and Dressler,[39] where a ratio of 1:8 was found for the electronic transition moments of the $GK \leftarrow B$ and $H\bar{H} \leftarrow B$ transitions at the equilibrium distance of the B-state. For transitions to Rydberg states with higher principal quantum numbers, the electronic transition moments are scaled in the same way as described for the doubly excited states. Using the Wigner–Eckart theorem and $\vec{\mu}_{\perp\pm} = (1/\sqrt{2})\langle\Pi|\vec{\mu}^+|\Sigma^\pm\rangle$,[40] it is derived that the electronic transition moment to $nd\pi_g$ states is 1.6 times smaller than that to $nd\sigma_g$ states:
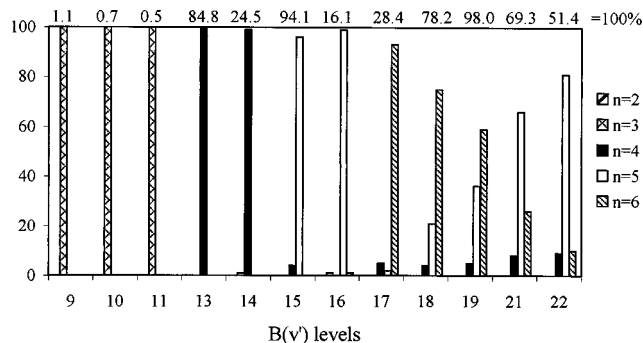
FIG. 7. Excited-atom distributions H(n) calculated for excitation via the $B\ ^1\Sigma_u^+(v')$ levels, and assuming that dissociation uniquely occurs by excitation of the vibrational continua of bound singly excited Rydberg states with $^1\Sigma_g^+(1s\sigma_g)(ns\sigma_g)$, $^1\Sigma_g^+(1s\sigma_g)(nd\sigma_g)$, and $^1\Pi_g(1s\sigma_g)(nd\pi_g)$ symmetry. For dissociation via each vibrational level, the sum of the cross sections for the pathways leading to H($n=2$) to H($n=6$) is set to 100% in the stick diagrams. The absolute value of this sum is given at the top of the diagram for each vibrational level.

$$\frac{\langle nd\sigma_g|\vec{\mu}_z|2p\sigma_u\rangle}{\frac{1}{\sqrt{2}}\langle nd\pi_g|\vec{\mu}^+|2p\sigma_u\rangle} = \frac{\begin{pmatrix}211\\000\end{pmatrix}}{-\frac{1}{\sqrt{2}}\begin{pmatrix}211\\-110\end{pmatrix}} = -1.6.$$

The probability for formation of H(n) is calculated by multiplying the Franck–Condon factor for excitation of the Rydberg state with principal quantum number n with the squared transition moments to $ns\sigma_g$, $nd\sigma_g$, and $nd\pi_g$, respectively, and by adding these contributions incoherently.

The simulation of the excited-atom distributions following from this mechanism is depicted in Fig. 7. The most striking difference from the previous model is that the contribution of H($n=2$) fragments to the distributions is now absent, in agreement with our experimental observations. These fragments can, within the present model, only be produced by excitation of the vibrational continuum of the $EF\ ^1\Sigma_g^+$ state, but our calculations indicate that the Franck–Condon factor for this pathway is negligibly small compared to excitation of the vibrational continua of $n=3$ and higher Rydberg states. This calculation also suggests that the closing down of the molecular ionization channel for excitation via $B\ ^1\Sigma_u^+(v'>8)$ levels, is due to the large cross section for excitation of the vibrational continua of the $n\geq3$ states in comparison with that for excitation of the $n=2$ states. Although the dominant features observed in photoionization and photodissociation are thus nicely reproduced, we notice that with this model, cross sections for H($n=3$) production via $v'=9–11$ are smaller than those obtained for H($n=2$) and H($n=3$) via the same transitions in the previous model (see Fig. 6 and 7). Quantitatively the agreement with the observed distributions is still poor. We note that a complete treatment has to combine the excitation of doubly excited repulsive curves, the excitation of the dissociation continua of bound Rydberg states, and the interactions between these states at large internuclear separations. We believe that these conclusions hold even if correct R-dependent electronic transition moments were employed.

IV. CONCLUSIONS

The photoionization and photodissociation dynamics occurring after one-photon absorption from several vibrational levels of the $B\ ^1\Sigma_u^+$ state, populated by three-photon excitation, were investigated by high-resolution photoelectron spectroscopy. The photoelectron spectra showed that absorption from the $v'=3–8$ levels of the $B\ ^1\Sigma_u^+$ state leads to both molecular photoionization and photodissociation. In this energy region it is, in particular, the molecular photoionization process which attracts attention. An *a priori* unexpected strong dependence of the vibrational and rotational branching ratios upon ionization was observed, which could only be rationalized if excitation of bound vibrational levels of singly excited Rydberg states at the four-photon level was taken into account.

For one-photon absorption from higher vibrational levels in the $B\ ^1\Sigma_u^+$ state ($v'\geq9$), the molecular photoionization pathway is completely suppressed, and only molecular photodissociation is observed. Furthermore, the $n=2$ dissociation channel effectively closes down. Dissociation into all other energetically allowed values of the principal quantum number n has been found up to H($n=14$), a cutoff which does not seem to be determined by the experimental technique but has to be determined by molecular properties.

The observed distributions have been compared with the results of two model calculations. In the first model, photodissociation is completely attributed to excitation of doubly excited states. Although the agreement between experiment and theory is not very satisfactory, these calculations allow us to conclude that not only the lowest doubly excited state plays a role in the dissociation dynamics, but also higher-lying repulsive states.

In the second model, dissociation occurs by excitation of the vibrational continua of singly excited Rydberg states. This model gratifyingly reproduces the closing down of the $n=2$ dissociation channel, and suggests that the suppression of the molecular ionization pathway for absorption from $v'\geq9$ levels is associated with the opening up of the $n=3$ dissociation channel. The model fails, however, in reproducing the distributions over the other n values. We note that quantitative agreement between experiment and this model can only be found if the interactions between doubly excited repulsive states and singly excited bound Rydberg states are taken into account. However, the present observations and calculations suggest that for one-photon absorption from vibrational levels with $v'\geq9$ of the $B\ ^1\Sigma_u^+$ state the predominant dissociation pathways may well arise from excitation of the vibrational continua of singly excited bound Rydberg states, rather than from excitation of doubly excited repulsive states.

ACKNOWLEDGEMENTS

J. Chem. Phys., Vol. 109, No. 19, 15 November 1998

Scheper *et al.* 8329

[1] W. A. Chupka, J. Chem. Phys. **87**, 1488 (1987).

[2] D. Zajfman, Z. Amitay, M. Lange, U. Hechtfischer, L. Knoll, D. Schwalm, R. Wester, A. Wolf, and X. Urbain, Phys. Rev. Lett. **79**, 1829 (1997).

[3] T. Tanabe, I. Katayama, N. Inoue, K. Chida, Y. Arakaki, T. Watanabe, M. Yoshizawa, S. Ohtani, and K. Noda, Phys. Rev. Lett. **70**, 42 (1993).

[4] P. Forck, M. Grieser, D. Habs, A. Lampert, R. Repnow, D. Schwalm, A. Wolf, and D. Zajfman, Phys. Rev. Lett. **70**, 426 (1993).

[5] M. Larsson, H. Danared, J. R. Mowat, P. Sigray, G. Sundström, L. Broström, A. Filevich, A. Källberg, S. Mannervik, K. G. Rensfelt, and S. Datz, Phys. Rev. Lett. **70**, 430 (1993).

[6] M. Larsson, M. Carlson, H. Danared, L. Broström, S. Mannervik, and G. Sundström, J. Phys. B **27**, 1397 (1994).

[7] D. Zajfman, Z. Amitay, C. Broudem, P. Forck, B. Seidel, M. Grieser, D. Habs, D. Schwalm, and A. Wolf, Phys. Rev. Lett. **75**, 814 (1995).

[8] W. J. van der Zande, J. Semaniak, V. Zengin, G. Sundström, S. Rosén, C. Strömholm, S. Datz, H. Danared, and M. Larsson, Phys. Rev. A **54**, 5010 (1996).

[9] S. T. Pratt, P. M. Dehmer, and J. L. Dehmer, J. Chem. Phys. **78**, 4315 (1983).

[10] J. H. M. Bonnie, J. W. J. Verschuur, H. J. Hopman, and H. B. van Linden van den Heuvell, Chem. Phys. Lett. **130**, 43 (1986).

[11] E. Y. Xu, T. Tsuboi, R. Kachru, and H. Helm, Phys. Rev. A **36**, 5645 (1987).

[12] J. W. J. Verschuur, L. D. Noordam, J. H. M. Bonnie, and H. B. van Linden van den Heuvell, Chem. Phys. Lett. **146**, 283 (1988).

[13] J. W. J. Verschuur and H. B. van Linden van den Heuvell, Chem. Phys. **129**, 1 (1989).

[14] S. T. Pratt, P. M. Dehmer, and J. L. Dehmer, Chem. Phys. Lett. **105**, 28 (1984).

[15] S. T. Pratt, P. M. Dehmer, and J. L. Dehmer, J. Chem. Phys. **85**, 3379 (1986).

[16] M. A. O'Halloran, S. T. Pratt, P. M. Dehmer, and J. L. Dehmer, J. Chem. Phys. **87**, 3288 (1987).

[17] S. T. Pratt, P. M. Dehmer, and J. L. Dehmer, J. Chem. Phys. **87**, 4423 (1987).

[18] C. W. Zucker and E. E. Eyler, J. Chem. Phys. **85**, 7180 (1986).

[19] D. Normand, C. Cornaggia, and J. Morellec, J. Phys. B **19**, 2881 (1986).

[20] C. Cornaggia, D. Normand, J. Morellec, G. Mainfray, and C. Manus, Phys. Rev. A **34**, 207 (1986).

[21] W. L. Glab and J. P. Hessler, Phys. Rev. A **35**, 2102 (1987).

[22] J. D. Buck, D. C. Robie, A. P. Hickman, D. J. Bamford, and W. K. Bischel, Phys. Rev. A **39**, 3932 (1989).

[23] E. Y. Xu, H. Helm, and R. Kachru, Phys. Rev. A **39**, 3979 (1989).

[24] E. Xu, A. P. Hickman, R. Kachru, T. Tsuboi, and H. Helm, Phys. Rev. A **40**, 7031 (1989).

[25] M. A. Buntine, D. P. Baldwin, and D. W. Chandler, J. Chem. Phys. **96**, 5843 (1992).

[26] E. F. McCormack, S. T. Pratt, P. M. Dehmer, and J. L. Dehmer, J. Chem. Phys. **98**, 8370 (1993).

[27] S. T. Pratt, P. M. Dehmer, and J. L. Dehmer, J. Chem. Phys. **86**, 1727 (1987).

[28] B. G. Koenders, D. M. Wieringa, K. E. Drabe, and C. A. de Lange, Chem. Phys. **118**, 113 (1987).

[29] C. E. Moore, *Atomic Energy Levels*, Natl. Bur. Stand. (U.S.) circ. 467, Vol. II (U.S. GPO, Washington, D.C., 1958).

[30] P. G. Wilkinson, Can. J. Phys. **46**, 1225 (1968).

[31] I. Dabrowski and G. Herzberg, Can. J. Phys. **52**, 1110 (1974).

[32] T. Namioka, J. Chem. Phys. **40**, 3154 (1964).

[33] J. Xie and R. N. Zare, J. Chem. Phys. **93**, 3033 (1990).

[34] D. L. Lynch, S. N. Dixit, and V. McKoy, Chem. Phys. Lett. **123**, 315 (1986).

[35] H. A. Bethe and E. E. Salpeter, *Quantum Mechanics of One and Two Electron Atoms* (Springer, Berlin 1957), section 70.

[36] L. D. Noordam, M. P. de Boer, and H. B. van Linden van den Heuvell, Phys. Rev. A **41**, 6267 (1990).

[37] S. L. Guberman, J. Chem. Phys. **78**, 1404 (1983).

[38] L. Wolniewicz, J. Phys. Chem. **51**, 5002 (1969).

[39] L. Wolniewicz and K. Dressler, J. Mol. Spectrosc. **96**, 195 (1982).

[40] H. Lefebvre-Brion and R. W. Field, *Perturbations in the Spectra of Diatomic Molecules* (Academic, Orlando, FL, 1986).